Contribution from the Department of Chemistry,
Texas A&M University, College Station, Texas 77843

Reactions of Dioxygen Complexes. Oxidative Dehydrogenation of 1,6-Bis(2-pyridyl)-2,5-diazahexane through Cobalt Dioxygen Complex Formation

Arup K. Basak and Arthur E. Martell*

Received December 1, 1987

The formation constants and oxygenation constants of the cobalt(II) complexes of 1,6-bis(2-pyridyl)-2,5-diazahexane (PYEN) have been determined by potentiometric equilibrium measurements under nitrogen and oxygen. The kinetics of the oxidative degradation of the coordinated ligand in the cobalt dioxygen complex have been measured spectrophotometrically, and the rate constants of two parallel degradation reactions have been determined. Both reactions were found to be second order, first order with respect to the concentration of the dioxygen complex and first order with respect to the hydroxide ion concentration. Kinetics and product analysis reveal that one of the terminal aminomethyl residues of the ligand PYEN undergoes two-electron oxidation to form the corresponding imine, which under the reaction conditions employed is converted to pyridine-2-carboxaldehyde, identified semiquantitatively as the (2,6-dinitrophenyl)hydrazone. Comparisons of these results with those of systems investigated previously, and the large kinetic deuterium isotope effect for the dehydrogenation reaction, are employed as the basis of a proposed reaction mechanism, which involves deprotonation of an aliphatic amino group in a preequilibrium step. The suggested rate-determining step in the proposed reaction mechanism involves concerted proton transfer from the α-carbons to the coordinated oxygens, homolytic O–O bond fission, formation of conjugated imine double bonds, and electron transfer through the metal ions from the α-C–N bond to coordinated dioxygen. The dioxygen is reduced to water (or coordinated hydroxide), and the cobalt remains in the divalent state.

Introduction

A number of dioxygen complexes formed from several cobalt(II)–polyamine complexes differ markedly in thermodynamic stabilities and cobalt–dioxygen bond strengths. Recent reviews[1-3] summarize the equilibria and kinetics of formation, electronic and vibrational spectra, magnetic properties, and crystal structures of cobalt dioxygen complexes. The cobalt dioxygen complexes formed in aqueous solution are usually binuclear and are usually represented as having a μ-peroxo bridge, while cobalt is generally indicated as essentially cobalt(III). A μ-hydroxo bridge also generally forms when less than five coordination sites are occupied by the coordinated ligand. Thus far, relatively limited data are available on the reactivities of these dioxygen complexes as oxidants for hydroxylation and oxidative dehydrogenation of organic compounds. Recently attention has been focused on the degradation reactions of μ-peroxo-bridged cobalt complexes to form inert cobalt(III) complexes, since the rates of such reactions are the limiting factors in the use of these complexes as intermediates in the catalytic oxidation and oxygenation of various substrates. Niederhoffer[4] has shown that cobalt(II) dioxygen complexes having ligands resistant to oxidation are converted to the corresponding inert cobalt(III) complexes with concomitant release of hydrogen peroxide. In some cases easily oxidizable coordinated ligands undergo oxidative dehydrogenation.[5,6] Dehydrogenation reactions of coordinated ligands are also found to occur[7-10] for the macrocyclic polyamine complexes of Ni^{2+}, Cu^{2+}, and Fe^{2+} with dioxygen, and these reactions are presumed to occur through dioxygen complex formation. It was found by Harris et al.[11,12] that binuclear cobalt dioxygen complexes with coordinated deprotonated dipeptides such as glycylglycine and their analogues undergo oxidative dehydrogenation at the N-terminal positions to form the corresponding imines. Recent reports from this laboratory[6,13] suggest that the autoxidation reactions are sensitive to the conformations of the coordinated ligands in the intermediate dioxygen complexes. A detailed study of the equilibria, kinetics, and mechanism for the oxidative dehydrogenation of 2-(aminomethyl)pyridine (AMP) by coordinated dioxygen in the dioxygen adduct formed from the mixed-ligand polyamine complex with diethylenetriamine (DIEN) and AMP has recently been published.[14] In order to further test the mechanisms suggested for oxidative dehydrogenation of coordinated pyridyl-containing polyamines in (mono) peroxo-bridged cobalt dioxygen complexes,[6,13] it was decided to undertake analogous studies of a dibridged μ-peroxo–μ-hydroxo cobalt dioxygen complex containing the tetraamine 1,6-bis(2-pyridyl)-2,5-diazahexane (PYEN). This paper describes the equilibria of dioxygen complex formation and the kinetics and mechanism of oxidative dehydrogenation of coordinated PYEN in its cobalt dioxygen complex.

Experimental Section

Materials. Reagent grade cobaltous nitrate was obtained from Fisher Scientific Co. and was used without further purification. Carbonate-free potassium hydroxide was obtained from J. T. Baker Chemical Co. and was used after dilution with carbon dioxide free, doubly distilled water. The exact concentration was determined by titration with potassium hydrogen phthalate with phenolphthalein as indicator. High-purity nitrogen, oxygen, and argon were obtained from AIRCO Gas Products Inc. and were used after the gases were passed through Ascarite and pyrogallol scrubbers (for nitrogen and argon) and through Ascarite (for oxygen) in order to remove trace impurities. The scrubbed gases were passed through and saturated with 0.100 M aqueous KNO_3 solution to prevent evaporation of water from the experimental solution.

1,6-Bis(2-pyridyl)-2,5-diazahexane, PYEN. *N,N'*-Ethylenebis(pyridine-2-carboxaldehyde imine) was prepared by the method of Busch and Bailar.[15] The Schiff base thus obtained was dissolved in ethanol and hydrogenated with 10% Pd–C as catalyst at 35 psi at room temperature. The catalyst was then filtered off, and the solvent was removed by vacuum evaporation. The brown oily residue was vacuum distilled in the temperature range 115–120 °C. The purity of the pale yellow oil obtained was verified by proton NMR spectroscopy in $CDCl_3$.

The yellow oil was dissolved in ethanol and treated with concentrated hydrochloric acid. The crystalline material obtained by cooling the solution was filtered off and washed with cold absolute ethanol until the filtrate was colorless. It was recrystallized twice from water containing a few drops of concentrated HCl. The colorless crystals of PYEN·4HCl were filtered off, washed with a small volume of very cold water, and finally dried under vacuum: mp 206 °C (lit. mp 208–208.5 °C[16]); yield 76%. ^1H NMR (in D_2O with excess KOD): δ 8.50 (2 H), 7.80 (2 H), 7.47 (4 H), 3.87 (4 H), 2.70 (4 H).

1,1,6,6-Tetradeuterio-1,6-bis(2-pyridyl)-2,5-diazahexane. α,α-Dideuterio-2-(aminomethyl)pyridine, prepared as described by Basak and

(1) Timmons, J. H.; Niederhoffer, E. C.; Martell, A. E. *Chem. Rev.* **1984**, *84*, 137.
(2) Jones, R. D.; Summerville, D.; Basolo, F. *Chem. Rev.* **1979**, *79*, 139.
(3) McLendon, G.; Martell, A. E. *Coord. Chem. Rev.* **1976**, *19*, 1.
(4) Niederhoffer, E. C. Ph.D. Dissertation, Texas A&M University, 1983.
(5) Martell, A. E. *Pure Appl. Chem.* **1983**, *55*, 125.
(6) Raleigh, C. J.; Martell, A. E. *Inorg. Chem.* **1985**, *24*, 142.
(7) Curtis, N. F. *J. Chem. Soc.* **1966**, 882; *Coord. Chem. Rev.* **1968**, *3*, 3.
(8) Dabrowiak, J. C.; Lovecchia, F. V.; Goedken, V. L.; Busch, D. H. *J. Am. Chem. Soc.* **1972**, *94*, 5502.
(9) Hipp, C. J.; Lindoy, L. F.; Busch, D. H. *Inorg. Chem.* **1972**, *11*, 1988.
(10) Goedken, V. L.; Busch, D. H. *J. Am. Chem. Soc.* **1972**, *94*, 7355.
(11) Harris, W. R.; Bess, R. C.; Martell, A. E.; Ridgeway, T. H. *J. Am. Chem. Soc.*, **1977**, *99*, 2958.
(12) Harris, W. R.; Martell, A. E. *J. Coord. Chem.* **1980**, *10*, 102.
(13) Raleigh, C. J.; Martell, A. E. *J. Coord. Chem.* **1985**, *14*, 113; *Inorg. Chem.* **1986**, *25*, 1190.
(14) Basak, A. K.; Martell, A. E. *Inorg. Chem.* **1986**, *25*, 1182.
(15) Busch, D. H.; Bailar, J. C., Jr. *J. Am. Chem. Soc.* **1956**, *78*, 1137.
(16) Lacoste, R. G.; Martell, A. E. *Inorg. Chem.* **1964**, *3*, 881.

0020-1669/88/1327-1948$01.50/0

Martell,[14] was dissolved in about 20 mL of water in a three-necked flask fitted with a condenser and magnetic stirrer. To this solution under an inert atmosphere of purified nitrogen were added 0.030 mol of $Ni(ClO_4)_2 \cdot 6H_2O$ in 5 mL of water and an equivalent (0.030 mol) amount of commercially available glyoxal (40% aqueous solution) in 40–50 mL of water, and the reaction mixture was stirred at room temperature for about 3 h. The solution was then cooled to about 5 °C, and to the stirred solution was added about 0.07–0.08 mol of $NaBH_4$ in small portions. The temperature of this reaction mixture was maintained at or below 5 °C; the mixture was then stirred, slowly brought to room temperature, and finally brought to the boiling point and filtered hot. After the filtrate was cooled, a yellow complex precipitated. The solid was filtered off and dissolved in water, excess solid KCN was added, and the solution was warmed to about 55–60 °C. The p[H] of the solution was adjusted to about 10.5–11.0. The liberated free base was extracted with chloroform. (Note: the chloroform extract was washed twice with water in order to remove any traces of perchlorate salt.) The chloroform extract was then dried with anhydrous Na_2SO_4, and the chloroform was stripped off to obtain the amine as a yellow oil. The oil was dissolved in absolute ethanol, concentrated hydrochloric acid was added, and the solution was chilled overnight. The colorless solid isolated was recrystallized twice from water acidified with HCl. The purity of the compound was checked by ^1H NMR spectroscopy and compared with the NMR spectrum of the nondeuteriated compound; yield ca. 27%. The absence of a proton NMR peak at 3.80 ppm clearly demonstrated that the α-carbon of the pyridine side chain was completely deuteriated; mp 209 °C. ^1H NMR (in D_2O with excess KOD): δ 8.60 (2 H), 7.80 (2 H), 7.50 (4 H), 2.63 (4 H).

2-(2,5-Diazapentyl)pyridine (EAMP). Pyridine-2-carboxaldehyde (9.5 mL, ca. 0.1 mol) was added dropwise to ethylenediamine (100 mL, ca. 1.5 mol) under a nitrogen atmosphere. The resulting mixture was refluxed for 3 h, and the reaction mixture was diluted with about 50 mL of absolute ethanol. To this solution was added excess solid $NaBH_4$ in small portions. The solution was then warmed to about 50–60 °C for approximately $1^1/_2$ h. After the solution was cooled to room temperature, it was filtered, and the filtrate was treated with about 100 mL of water. The aqueous solution having a pH of approximately 10.7 was extracted with chloroform. The chloroform solution was dried with anhydrous Na_2SO_4, the chloroform was removed by vacuum evaporation, and a yellow oil was obtained. It was distilled under vacuum, and the fraction distilling at 100–105 °C was dissolved in concentrated hydrochloric acid. The solid hydrochloride was obtained after the reaction mixture was cooled for 2 days. ^1H NMR for EAMP·3HCl (D_2O with three drops of 40% KOD solution): δ 8.53 (1 H), 7.82 (1 H), 7.47 (2 H), 3.82 (2 H), 2.73 (4 H). Yield: ca. 42%.

Anal. Calcd for $C_8H_{16}N_3Cl_3$: C, 36.80; H, 6.19; N, 16.13. Found: C, 36.52; H, 6.17; N, 16.18.

Potentiometric Equilibrium Determinations. A Co(II) solution having a concentration of about 0.10 M was prepared from reagent grade cobaltous nitrate and was standardized by direct titration with standard ethylenediaminetetraacetic acid disodium salt (EDTA) with Murexide as indicator.[17] A Corning Model 130 digital pH meter was used to determine the hydrogen ion concentrations in all potentiometric measurements, which were carried out in a jacketed vessel maintained at 25.00 ± 0.01 °C by circulation of thermostated water. The potentiometric cell was equipped with a Sargent Welch glass electrode, calomel reference electrode, gas inlet, bubbler outlet, and graduated (Metrohm) microburet. The electrode assembly and the pH meter were calibrated with standard aqueous HCl and KOH solution to read $-\log [H^+]$ directly. In order to maintain the linearity of the EMF–hydrogen ion calibration it was essential that the free $[H^+]$ and $[OH^-]$ be limited to a very small fraction of that of the supporting electrolyte. This limitation restricts the $-\log [H^+]$ measurements to the range 2–12. For the purposes of this paper, $-\log [H^+]$ is designated by the term p[H].

The ionic strength of the medium was maintained at 0.100 M by addition of standard KNO_3 solution. The potentiometric measurements were carried out under an atmosphere of purified nitrogen and oxygen, respectively. For the potentiometric measurements at 25.0 °C the following solutions were measured. Anaerobic solutions (under N_2): $[PYEN \cdot 4HCl] = 3.194 \times 10^{-3}$ M; $[PYEN \cdot 4HCl] = [Co^{2+}] = 2.466 \times 10^{-3}$ M. Aerobic solution (1.00 atm of O_2): $[PYEN \cdot 4HCl] = 2.318 \times 10^{-3}$ M, $[Co^{2+}] = 2.250 \times 10^{-3}$ M.

The protonation constants of the ligand were calculated with the aid of the program PKAS.[18] The stability constants of the metal chelates and hydrolysis products and the equilibrium constants for the formation of the oxygen adducts and the hydrolyzed oxygen adducts were calculated with the aid of the computer program BEST.[19] The methods used for computation are the same as those described earlier.[20] Species distribution curves for the 1:1 M:L system under nitrogen and oxygen were generated with the aid of a FORTRAN computer program SPE written by Dr. R. J. Motekaitis of this laboratory.

The UV–visible absorption spectra of the complexes were recorded with a Perkin-Elmer Model 553 fast-scan spectrophotometer equipped with a remote-control time-drive chart recorder and with matched quartz cells of path length 1.000 ± 0.001 cm. Proton NMR spectra were measured on a Varian EM-390 90-MHz spectrometer.

Reaction Kinetics. The kinetics of decomposition of the dioxygen complex was monitored by following the decrease in absorbance of the ligand-to-metal charge-transfer band ($\pi_{O_2}^* \rightarrow d_{z^2}$) at 380 nm, where there is maximum difference in absorbance between the product and the reactant. The kinetic data determined are the mean of at least three separate kinetic runs. Anaerobic conditions were maintained throughout the kinetic runs in order to avoid the reoxygenation of the cobalt(II) complex formed in the reaction. The temperature coefficient data necessary for calculating activation parameters were determined by measuring reaction rates at 5 °C intervals between 45 and 60 °C.

Product Identification of First Oxygenation-Degradation Cycle. In separate experiments 1.005×10^{-3} M dioxygen complex was digested at 50.0 °C at pH 11.88 for about 5–6 half-lives until the UV–visible absorbance attained a constant value. Then a measured volume of this solution was treated with an acidic solution of (2,4-dinitrophenyl)hydrazine (5% excess) in order to determine quantitatively the amount of pyridine-2-carboxaldehyde formed in situ by hydrolysis of the imine formed from the first dehydrogenation cycle of the dioxygen complex. The yellow crystalline product obtained was filtered and washed repeatedly with water until the washings were colorless. It was dried and weighed as the (2,4-dinitrophenyl)hydrazone derivative of pyridine-2-carboxaldehyde. The weight of the derivative corresponds to about 2 equiv of aldehyde within the limit of experimental error. Found: (1) 1.81 equiv; (2) 1.84 equiv; (3) 1.79 equiv.

Results and Discussion

Synthetic Methods. The ligand PYEN was synthesized by the method previously reported by Lacoste and Martell.[16] The triamine, EAMP, which seems to be a new compound, was prepared by an analogous procedure in ca. 42% yield.

After several methods were considered for the synthesis of 1,1,6,6-tetradeuteriated PYEN, it appeared that the best is the metal-template reaction described by Nakamura et al.,[21] which involves the condensation of glyoxal with pyrrolidin-2-ylmethylamine in the presence of metal chloride to form the corresponding tetradentate diimine chelate. Kaden[22] also reported a synthetic route consisting of the condensation of glyoxal with open-chain amines through the use of a metal-template reaction. On the basis of this prior work on nondeuteriated compounds, 1,1,6,6-perdeuteriated PYEN was synthesized by the use of a α,α-dideuterio-2-(aminomethyl)pyridine:glyoxal:nickel perchlorate hexahydrate 2:1:1 molar ratio. The imine complex thus formed was successfully reduced with $NaBH_4$, and the yellow Ni(II) complex of the tetraamine was isolated. The nickel(II) was removed with excess potassium cyanide, and the free amine was extracted from basic solution by extraction with chloroform in ca. 27% yield.

Thermodynamic Stabilities. Potentiometric equilibrium curves of 1,6-bis(2-pyridyl)-2,5-diazahexane, PYEN, in the absence and in the presence of an equivalent amount of cobalt(II) under nitrogen and oxygen are shown in Figure 1. The top curve (PYEN·4HCl alone, L) shows a low-pH two-proton buffer region followed by three inflections at a = 2.0, 3.0, and 4.0 mol of base/mol of ligand. The calculated protonation constants for the ligand are $\log K_4^H = 0.6 \pm 0.05$, $\log K_3^H = 1.35 \pm 0.05$, $\log K_2^H = 5.45 \pm 0.01$, and $\log K_1^H = 8.390 \pm 0.005$ at 25.0 °C and at ionic strength 0.100 M (KNO_3). The high acidities of the tetrapositive and tripositive ions of PYEN are considered due to the low proton affinities of the pyridyl groups.

(17) Schwarzenbach, G. *Complexometric Titration*; Methuen: London, 1957; p 78.
(18) Motekaitis, R. J.; Martell, A. E. *Can. J. Chem.* **1982**, *60*, 168.
(19) Motekaitis, R. J.; Martell, A. E. *Can. J. Chem.* **1982**, *60*, 2403.
(20) Taliaferro, C. H.; Motekaitis, R. J.; Martell, A. E. *Inorg. Chem.* **1984**, *23*, 1188.
(21) Nakamura, A.; Mori, Y.; Oguni, N. *J. Chem. Soc., Dalton Trans.* **1982**, 2359.
(22) Kaden, T. A., personal communication. Schibler, W. Ph.D. Dissertation, Universitat Basel, Basel, Switzerland, 1980.

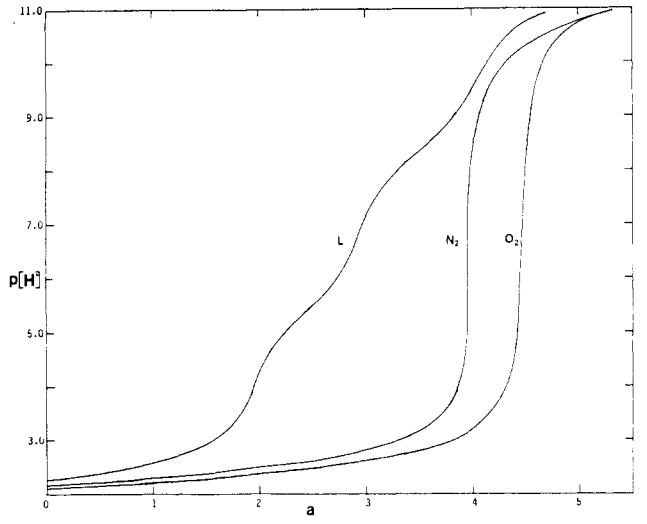

Figure 1. Potentiometric equilibrium curves for a 1:1 molar ratio of PYEN to Co(II) under N_2 and O_2 (25.00 ± 0.05 °C, μ = 0.100 M (KNO_3); a is the number of moles of base added per mole of ligand): L, PYEN·4HCl; N_2, 1:1 PYEN·4HCl:Co(II) system under N_2; O_2, 1:1 PYEN·4HCl:Co(II) system under 1.00 atm of O_2.

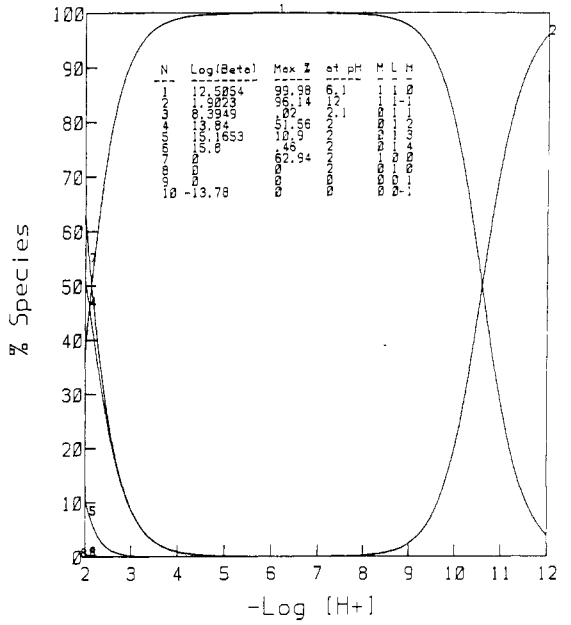

Figure 2. Species distribution vs p[H] of the 1:1 Co(II):PYEN system (2.466×10^{-3} M) under N_2 (25.00 °C, μ = 0.100 M (KNO_3)).

The 1:1 ligand to cobalt(II) ion equilibrium curve, N_2, has a long buffer zone terminated by a sharp inflection at a = 4.0. At p[H] 8–9 the curve shifts to higher a values, indicating reaction with more alkali as a result of a hydrolytic reaction of the complex CoL^{2+}. The lowering of the potentiometric titration curve even at the initial p[H] relative to that of the ligand alone indicates that metal–ligand complex formation starts at the lowest p[H] measured potentiometrically. From the species distribution curve of the system under nitrogen (Figure 2) it appears that formation of the 1:1 metal:ligand complex, ML, is complete at p[H] 4.5. The ligand occupies four coordination sites of the metal ion, with the possibility of hydrolysis at the remaining aquo sites. Above p[H] 8.0 the concentration of the hydroxo complex starts to increase, and at p[H] 10.5 the concentrations of ML^{2+} and $ML(OH)^+$ are nearly equivalent.

The potentiometric equilibrium curve for the 1:1 $[Co^{2+}]$:[PYEN] system under an oxygen atmosphere shows a further drop in p[H] of the buffer region, which is terminated by a sharp inflection at a = 4.5, indicating the additional amount of base needed for the formation of the oxygenated species. The equivalence point observed indicates the formation of a binuclear

Table I. Equilibrium Constants for PYEN and Its Cobalt Complexes (1:1) under Nitrogen and Oxygen (25.0 °C, μ = 0.100 M (KNO_3))

ion	quotient, Q	log Q^a	log Q^b	ref
H^+	$[HL^+]/([H^+][L])$	8.39	8.23	16
	$[H_2L^{2+}]/([H^+][HL^+])$	5.45	5.45	16
	$[H_3L^{3+}]/([H^+][H_2L^{2+}])$	1.3	1.81	16
	$[H_4L^{4+}]/([H^+][H_3L^{3+}])$	0.6	1.62	16
Co^{2+} (under N_2)	$[CoL^{2+}]/([Co^{2+}][L])$	12.51	12.80	16
			11.96	23
	$[CoL^{2+}]/([CoL(OH)^+][H^+])$	10.61		
Co^{2+} (under O_2)	$[(Co_2L_2(O_2^{2-})(OH^-))^{3+}][H^+]/([CoL^{2+}]^2[O_2]$	1.37		

[a] This work. [b] Other work (see references).

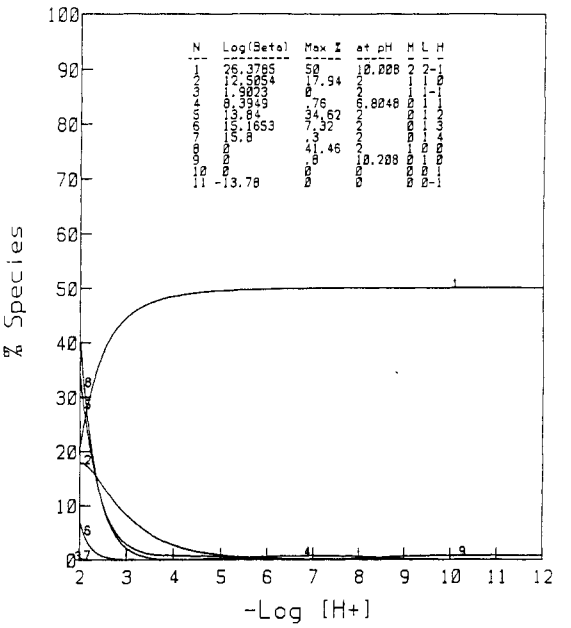

Figure 3. Species distribution vs p[H] of the 1:1 Co(II):PYEN system (2.250×10^{-3} M:2.318×10^{-3} M) under O_2 (25.00 °C, μ = 0.100 M (KNO_3)).

complex with μ-peroxo and μ-hydroxo bridging. The stability constants and protonation constants calculated from the potentiometric equilibrium data, given in Table I, agree reasonably well with those reported earlier.[16,23] Current values are considered more precise because of improvement in instrumentation, method of calculation, and the purity of the ligand.

The species distribution curve of the 1:1 Co^{2+}:PYEN system under oxygen (Figure 3) indicates that above p[H] 4.5 the di-bridged dioxygen complex is the major species and above p[H] 5.0 it is virtually the only species present in solution. The suggested coordinate bonding in this dioxygen complex is illustrated by **1**.

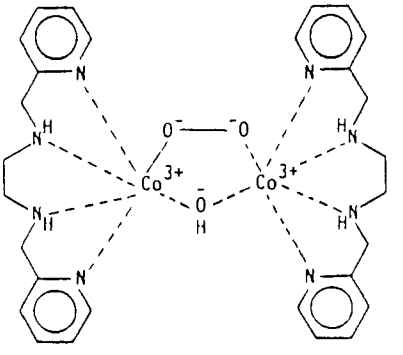

1, $Co_2(PYEN)_2(O_2)(OH)^{3+}$

(23) Anderegg, G.; Podder, N. G.; Plauenstein, P.; Hangartner, M.; Stunzi, H. *J. Coord. Chem.* **1975**, *4*, 267.

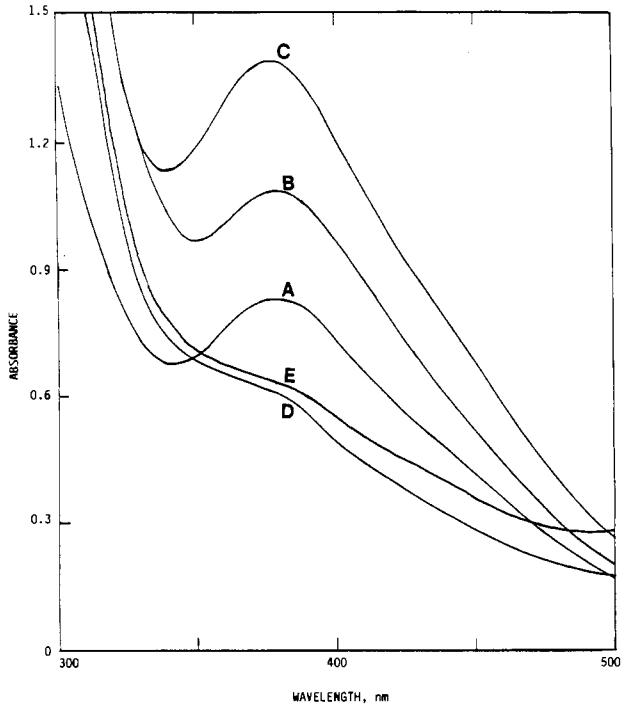

Figure 4. UV–vis spectra of PYEN complexes: A, $Co^{II}(H_2O)_2(PYEN)$ (2.026×10^{-3} M, p[H] 5.0); B, $Co^{II}(OH)(H_2O)(PYEN)$ (1.885×10^{-3} M, p[H] 11.5); C, $Co_2(\mu\text{-}O_2)(\mu\text{-}OH)(PYEN)_2$ (2.088×10^{-4} M, p[H] 10.8); D, product obtained after complete decomposition of the dibridged dioxygen complex at p[H] 11.7 and 50.0 °C under anaerobic conditions; E, 1:1:1 Co(II):PYEN:Pyridine-2-carboxaldehyde system under N_2 (p[H] 11.7, 4.176×10^{-4} M).

Table II. UV–Visible Absorption Characteristics of Cobalt Complexes of PYEN (25.0 °C, μ = 0.100 M (KNO_3))

complex	p[H]	λ_{max}, nm	ϵ_{max}, M^{-1} cm^{-1}
$CoL(OH_2)_2^{2+}$	4.97	378	415
$CoL(OH)(OH_2)^{+}$	11.54	378	548
$Co_2L_2(O_2^{2-})(OH)^{3+}$	10.77	375	7145

The UV–visible spectra of the complexes $Co(PYEN)(OH_2)_2^{2+}$, $Co(PYEN)(OH)(OH_2)^{+}$, and $Co_2(PYEN)_2(O_2)(OH)^{3+}$ are illustrated in Figure 4, and the molar absorbances measured for the complexes are reported in Table II.

Kinetics. At 50.0 °C, the absorbance of the μ-peroxo–μ-hydroxo Co(III)–PYEN complex, from which all excess dioxygen has been removed, was observed to decrease rapidly with time at high p[H] and more slowly at lower p[H] values. The intense absorption band at 380 nm, which decreases in absorbance with time, is assigned to the ligand-to-metal charge transfer, LMCT, $\pi_{O_2}^* \rightarrow d_{z^2}$ for the dibridged cobalt–dioxygen complex. From product analysis it was found that after the first dehydrogenation reaction, the coordinated imine formed hydrolyzes to give pyridine-2-carboxaldehyde.

The kinetics of dehydrogenation of the dioxygen complex was monitored by following the decrease in absorbance in the p[H] range 11–12 under anaerobic conditions at 380 nm (Figure 5). The first-order plot of $-\log (A_t - A_\infty)$ vs time was not linear throughout the total reaction time. There are two seemingly linear sections with a definite break between the initial time period and subsequent longer time interval, which suggests that the degradation reaction consists of at least two reactions, which may occur successively or simultaneously. Alternatively the nonlinear semilog plots might be due to the second-order dependence on the initial complex concentration. In separate experiments it was found that at fixed p[H] the degradation rate constants are linearly dependent on dioxygen complex concentration with a slope of 0.97 (first-order in complex concentration), which eliminates the possibility of the alternative intermolecular pathway for ligand oxidation.

In a system with reaction pathways such as $A \xrightarrow{k^f} C$ and $B \xrightarrow{k^s} C$ ($k^f > k^s$), where C is the reaction product and A and B are two

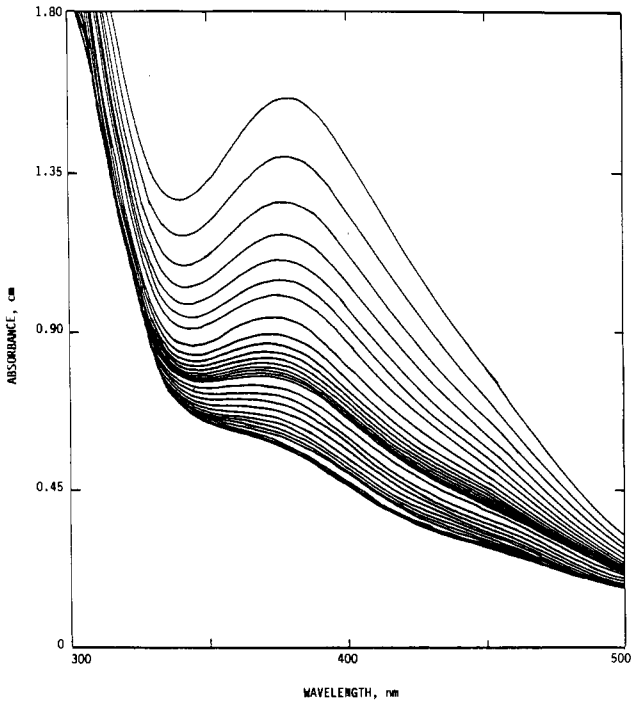

Figure 5. Spectral scans for the decomposition of the μ-peroxo–μ-hydroxo Co(II) PYEN complex at p[H] 11.90 (50.0 °C, μ = 0.100 M (KNO_3), [O_2 complex] = 2.088×10^{-4} M, Δt = 25 min for the first 17 scans and then Δt = 100 min).

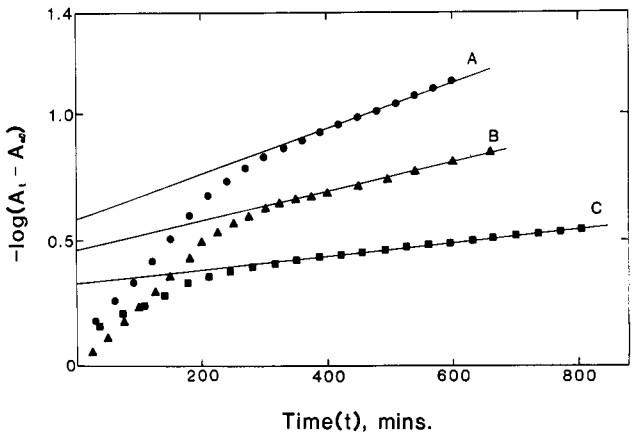

Figure 6. Plot of $-\log (A_t - A_\infty)$ vs time, t, for evaluation of k_{obsd}^s (50 °C, μ = 0.100 M (KNO_3)). p[H]: A, 11.90; B, 11.81; C, 11.47.

reactants that form the same product, the data near the end of the overall reaction time may be considered as indicating a simple conversion of B to C. On that basis the rate constant for the slow reaction was computed from the slope of the linear portion of the plot of $-\log (A_t - A_\infty)$ vs time t for the second linear time interval. Figure 6 is a representative example of such a plot at three p[H] values. The same method was used for evaluating the rate constants for the slow step at other p[H] values, at other temperatures, and for the corresponding PYEN-1,1,6,6-d_4 system. The results obtained are reported in Tables III and IV.

The rate constants for the initial part of the reaction were evaluated from the slope of the plot $-\log [(A_t - A_\infty) - (A_t - A_\infty)']$ vs time over the initial time period, where $(A_t - A_\infty)'$ was obtained by extrapolating the linear portion of the long time data to zero time, thus providing correction factors for the initial rate constants. The graphical evaluation of k_{obsd} for the fast reaction at several p[H] values is shown in Figure 7. The plots of log k_{obsd} for both the "fast" and "slow" reactions are linearly dependent on p[H] of the reacting solution (Figure 8) with a slope of unity, clearly indicating that both reactions have first-order dependence on hydroxide ion concentration. The second-order rate constants were

Table III. Pseudo-First-Order Rate Constants, k_{obsd}, and Second-Order Rate Constants for the Decomposition of the Dioxygen Complexes Formed from Co(II) and PYEN under Anaerobic Conditions as a Function of p[H] (50.0 °C, μ = 0.100 M (KNO_3))

ligand	p[H]	$10^2[OH^-]$, M[a]	$10^5 k_{obsd}^{init}$, s^{-1} [b]	$10^5 k_{obsd}^{final}$, s^{-1}	$10^4 k_1^s$, M^{-1} s^{-1}	$10^4 k_1^f$, M^{-1} s^{-1}
PYEN	11.90	7.93	20.73	3.46		
	11.81	6.50	17.15	2.23		
	11.47	2.97	9.33	1.02	3.85	22.11
	11.37	2.32	6.23	0.97		
	11.32	2.10	5.42	0.77		
	11.12	1.31	3.95	0.55		
PYEN-*1,1,6,6-d*$_4$	11.91	8.13	2.66	0.41		
	11.80	6.31	2.03	0.30	0.52 (7.4)	2.71 (8.2)
	11.47	2.97	0.5	0.10		

[a] Values of $[OH^-]$ were calculated by assuming pK_w = 13.00 at 50.0 °C and μ = 0.100 M (KNO_3). [b] $k_{obsd}^{init} = k_1^f[OH^-] + k_1^s[OH^-]$; $k_{obsd}^{final} = k_1^s[OH^-]$ (see text). [c] Figures in parentheses represent the kinetic isotope effects.

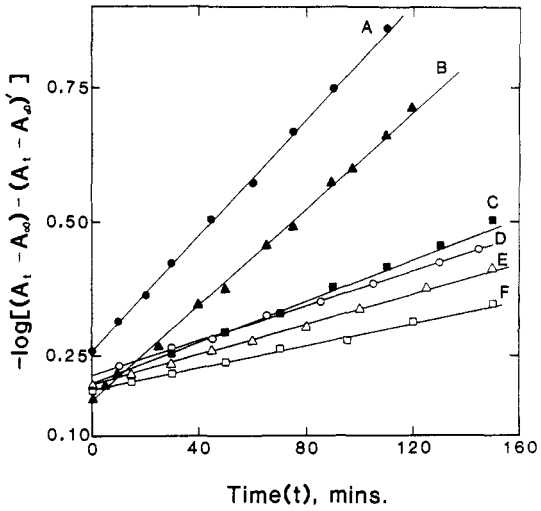

Figure 7. Plot of $-\log [(A_t - A_\infty) - (A_t - A_\infty)']$ vs time (initial time period) for evaluation of k_{obsd}^f (50 °C, μ = 0.100 M (KNO_3)). p[H]: A, 11.90; B, 11.81; C, 11.47; D, 11.37; E, 11.32; F, 11.12.

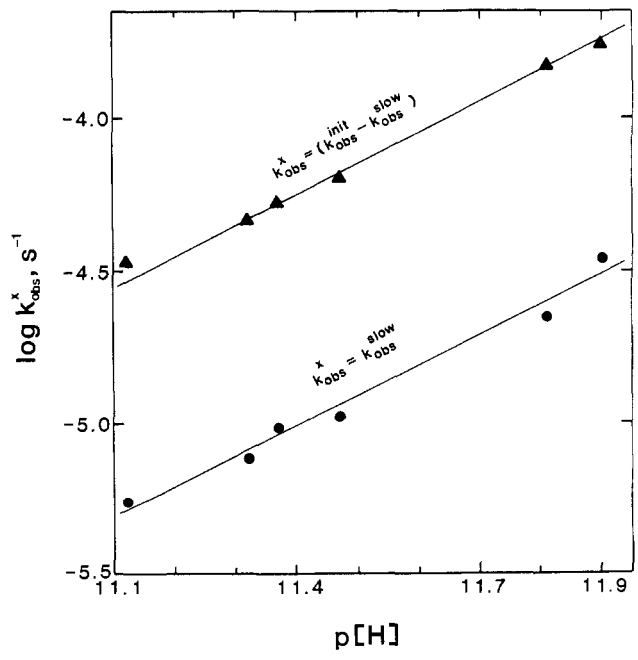

Figure 8. Dependence of pseudo-first-order rate constants on p[H] for the fast step and slow step (50.0 °C, μ = 0.100 M (KNO_3)).

evaluated from the plot of k_{obsd}^x (where x = "f" or "s") vs $[OH^-]$ for both PYEN and PYEN-1,1,6,6-d_4 (Figure 9) and are listed in Table III. The differences in the observed rate constants for the "slow" and "fast" steps indicate that the slow process does not affect the fast process.

Table IV. Activation Parameters for Fast and Slow Steps[a]

temp, °C	$10^4 T^{-1}$, K^{-1}	$10^4 k_1^s$, M^{-1} s^{-1}	$10^4 k_1^f$, M^{-1} s^{-1}
45	31.45	1.32	10.51
50	30.96	3.85	22.10
55	30.49	9.98	41.72
60	30.03	24.60	72.10
ΔH^*, kcal/mol		40.4	26.4
ΔS^*, eu		+50.3	+10.4

[a] Activation parameters were calculated by using the Eyring equations: $-\log [k_1^x(h/kT)] = \Delta H^*/4.6T - \Delta S^*/4.6$ (where x = f or s).

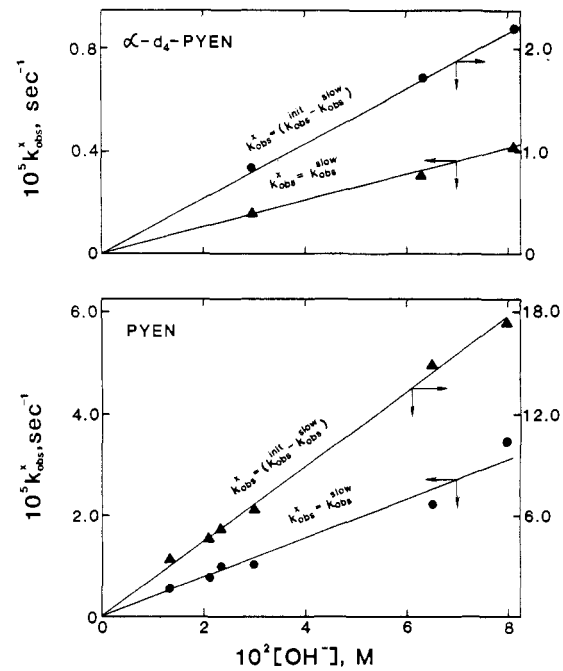

Figure 9. Evaluation of second-order rate constants for both slow and fast steps, k^s and k^f, for the ligands PYEN and PYEN-1,1,6,6-d_4 (50.0 °C, μ = 0.100 M (KNO_3)).

The observed rate behavior for the degradation of the dioxygen complex is described by eq 1–5.

$$-\frac{d[A]}{dt} = k_1^f[OH^-][A] \quad (1)$$

$$-\frac{d[B]}{dt} = k_1^s[OH^-][B] \quad (2)$$

so that

$$-\frac{d[complex]}{dt} = k_{obsd}^j[complex] = -\frac{d[A]}{dt} - \frac{d[B]}{dt} \quad (3)$$

where [complex] = total complex concentration consisting of all isomeric forms of the dioxygen complex present in solution. For the early stage

$$k_{obsd}^{init} = (k_1^f[A] + k_1^s[B])[OH^-] \quad (4)$$

Chart I. Isomeric Forms of the Dibridged Cobalt PYEN Dioxygen Complex

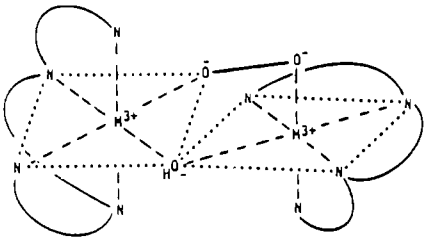

2 Both pairs of coplanar rings cis to dioxygen

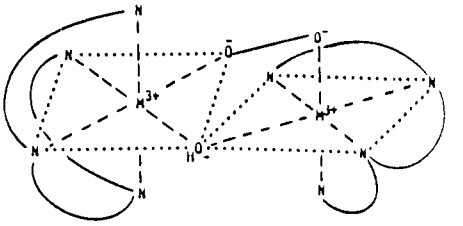

3 One pair of coplanar rings trans and other pair cis to dioxygen

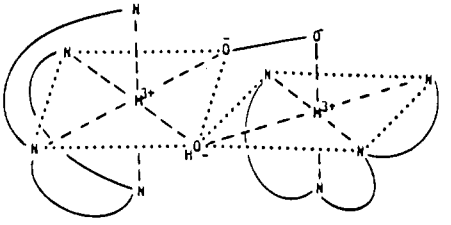

4 Both coplanar pairs of rings trans to coordinated dioxygen

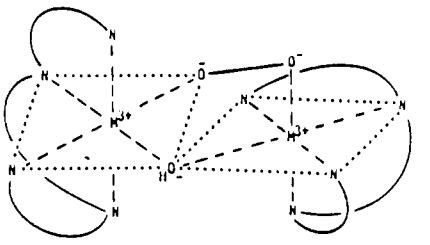

5 One pair of coplanar rings cis to dioxygen; other ligand folded

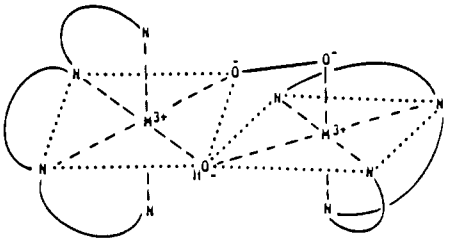

6 Both ligands folded

For the final period, when the more reactive component is no longer present

$$k_{obsd}^{final} = k_1^s[OH^-] \quad (5)$$

Deuterium Isotope Effect. In order to determine the deuterium isotope effect, the kinetics of decomposition of the dibridged dioxygen complex formed by PYEN-1,1,6,6-d_4 was measured at the same temperature, ionic strength, and pH range as that described above for the hydrogen analogue. The values of pseudo-first-order rate constants, both initial and final, for both PYEN and PYEN-1,1,6,6-d_4 are reported in Table III. The second-order rate constants obtained for both fast and slow steps along with the corresponding deuterium isotope effects are presented in Table III.

Reaction Pathways. With two distinctly different rates of degradation, there is the question of the selection from among the following possible reaction pathways I–IV. (The kinetic analysis given above is clearly pathway III.) If A and B are in

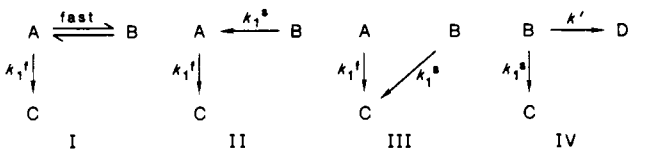

rapid equilibrium, only one rate would be detected, so that pathway I may be eliminated. Again, if one assumes that B is reactive and if, while undergoing decomposition, this reactive form produces a "dead-end intermediate" D, as is sometimes observed in enzyme kinetics,[24] then the "dead-end intermediate" D does not undergo the degradation reaction. However, the nearly quantitative formation of 2 equiv of aldehyde, observed in product analysis, provides strong evidence for the elimination of pathway IV.

There seems to be no way to make a selection between II and III on the basis of observed kinetics alone. Initially, the second pathway was tentatively selected. This assumed that all of the observed reaction must go through A and that the slow step involves rate-determining conversion of B to A. The alternative assumes that isomers A and B are not interconvertible in the time scale of the observed kinetics and that A and B are converted to C by parallel but independent pathways. The magnitude of the kinetic deuterium isotope effect for the slow step, which is very large and nearly as large as (i.e., not significantly different from) that of the fast step, makes it impossible that this step be a simple isomerization (B → A), as in pathway II, but must also involve hydrogen transfer from carbon to oxygen, as in III. Thus A → C and B → C are similar reaction types, and pathway III is selected as the slow step.

A search for the probable reason for the fast and slow steps for the oxidative dehydrogenation reaction leads to consideration of the possible stereochemical arrangements of the tetradentate ligand (PYEN) surrounding each cobalt atom in the dibridged dioxygen complex. In this case the existence of the hydroxo bridge, and the requirement that it be cis to the peroxo bridge, greatly restricts the total number of possible conformers. Formulas **2–6** (Chart I) illustrate the possible orientations of the coordinated ligand relative to the peroxo bridge.

Dehydrogenation Mechanism. Comparison of the conformations of the coordinated ligands in **2–6**, in the light of two distinctly

(24) Cleland, W. W. In *Investigation of Rates and Mechanisms of Reactions*, Bernasconi, C. F., Ed.; Wiley: New York, 1986; Part I, p 810.

(25) Raleigh, C. J.; Martell, A. E. *J. Chem. Soc., Chem. Commun.* **1984**, 335.

different rates of oxidative dehydrogenation, reveals a situation that is quite analogous to the observations and interpretations of Raleigh and Martell[6,13,24] for the kinetics of oxidative dehydrogenation of pentadentate pyridyl-containing polyamines coordinated to cobalt in the corresponding dioxygen complexes. It was observed[13,24] that one of the requirements for facile oxidative deamination to the corresponding coordinated imines is that the chelate ring containing the α-aminomethyl group, the adjacent pyridine nitrogen, and the adjacent chelate ring involving the two aliphatic amino nitrogen donors need to be approximately coplanar in order to allow the generation of the trigonal α-imine nitrogen without breaking a cobalt–nitrogen coordinate bond. It is seen that these requirements are met in formula **2**, and a low-energy pathway exists for the generation of one α-imine group in each coordinated ligand. The folded conformation of both ligands in **6**, however, would prevent, or greatly reduce the rate of, oxidative dehydrogenation to the coordinated imine without prior rearrangement of the coordinate bonds. Thus, it seems the formula **2** probably represents the conformation of the isomer that undergoes the more rapid rate of oxidative dehydrogenation.

There are other possible conformations, **3**–**5**, that should also be considered. In **3** and **4** it is seen that the requirement of two approximately coplanar chelate rings is satisfied. However, in **4** the α-amino groups to be dehydrogenated are probably too far from the coordinated dioxygen to allow facile transfer of an α-proton to the coordinated dioxygen, which is one of the requirements for homolytic O–O fission (this requirement is discussed further below). It would seem, therefore, that conformer **4** would not undergo oxidative dehydrogenation or at least would undergo such a reaction much more slowly than would the isomeric complex **2**. In complex **3**, however, one set of coplanar chelate rings is close to the peroxo bridge while the other is farther away. Perhaps in this case oxidative dehydrogenation could take place *albeit* at a slower rate than that of **2**. In the case of **5** the presence of a completely folded structure for one of the chelate ligands would prevent a concerted dehydrogenation mechanism, with accompanying homolytic O–O fission. Thus, **5** would not undergo facile oxidative dehydrogenation if the concerted mechanism is a requirement. The relative distances between the groups undergoing dehydrogenation and the coordinated dioxygen, described above on the basis of qualitative comparisons of formulas **2**–**6**, is further supported by the use of space-filling CPK[26] models.

The activation entropies and enthalpies for both the fast and slow steps have been determined by measuring the rates of the dehydrogenation reaction in the temperature range 45–60 °C. Activation parameters were determined graphically (Figure 10) by use of the Eyring relationship.[27] The temperature variations of k_1^s and k_1^f, along with activation parameters ΔH^* and ΔS^*, are presented in Table IV.

For the fast step the activation enthalpy is 26.4 kcal/mol so that E_a for the fast step is ca. 27 kcal/mol, which is similar in magnitude to that reported previously[6] for the oxidative dehydrogenation reaction of the dioxygen complex formed by cobalt(II), PYDIEN (i.e., 1,9-bis(2-pyridyl)-2,5,8-triazanonane), and oxygen (E_a = 29.3 kcal/mol). Comparison of the activation energies of these two processes supports the suggestion made earlier[14] that the cleavage of the C–H and O–O bonds is concerted, as represented by transition state **8** in Scheme I.

It was found that the ΔS^* value for the slow step is much higher than that found for the fast step. This suggests that the more reactive isomer (formula **2**) is sterically more favorable to the formation of a transition-state structure such as **8** and suggests a higher entropy of activation for the slow step. Hence, the reorganization of the dibridged dioxygen complex to allow proton and electron transfer is an important factor controlling the rate of oxidative dehydrogenation.

The suggestion that structure **2** has the more favorable stereochemistry to facilitate the transfer of electrons to the dioxygen through the coordinated metal ion, as indicated in the proposed transition state **8**, once again indicates that a controlling factor for oxidative dehydrogenation of the coordinated polyamine is found in the stereochemistry of the dioxygen complex, and depends to a large extent on proximity of the part of the ligand undergoing dehydrogenation to the coordinated dioxygen, as well as on the conformation of the coordinated ligand itself.

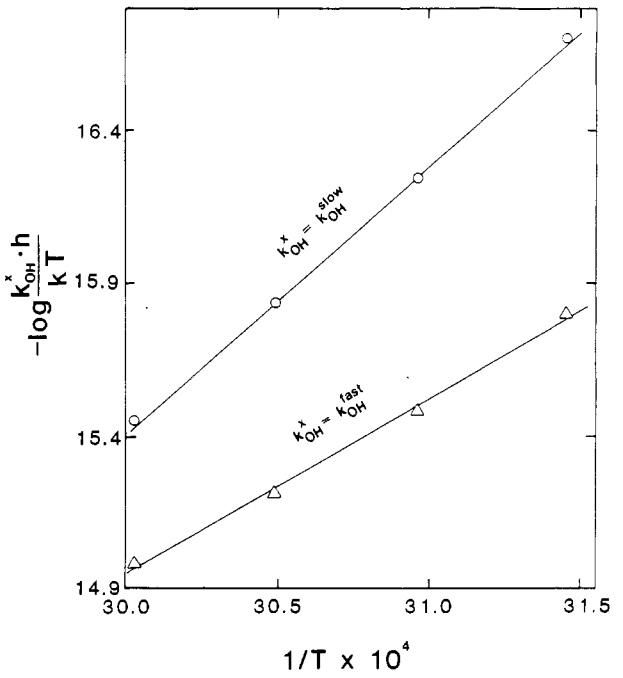

Figure 10. Evaluation of activation parameters for both slow and fast steps (h = Planck's constant, k = Boltzmann's constant, T in kelvin).

Comparison of the rate constants for the oxidative dehydrogenation of the coordinated ligand in this dioxygen complex with other μ-peroxo-bridged cobalt complexes having coordinated pentadentate polyamine ligands described previously shows that for the present system the activation energy is considerably higher. This increased activation energy could be the result of greater steric restraints on the conformation(s) of the dioxygen complexes imposed by the double μ-peroxo–μ-hydroxo bridge. This interpretation seems to be in conformity with the absence of a hydroxide ion independent path for oxidative dehydrogenation in the present system compared to other ternary complex systems, for which both hydroxide ion dependent and hydroxide ion independent pathways were observed.[14] The slow rate of oxidative dehydrogenation of the dibridged complex compared to that of the monobridged complex reported earlier[6,13,14] is probably due to steric requirements and the necessity of breaking the hydroxo bridge before electron transfer can occur.

Product analysis indicates that, as a result of oxidative dehydrogenation, one (aminomethyl)pyridine moiety of each of the two ligands present in the complex is converted to the imine, which subsequently hydrolyzes to the corresponding aldehyde. Thus the overall dehydrogenation reaction proceeds by a four-electron transfer to give a single reaction product. The linear dependence of the pseudo-first-order rate constant on p[H] suggests the possibility of base-assisted opening of the hydroxo bridge resulting in an intermediate with a deprotonated nitrogen on each metal ion, as indicated in Scheme I. Deprotonation of the coordinated nitrogens, illustrated by **7**, would assist electron transfer to the dioxygen through the coordinated metal ion. On the basis of these experimental observations, it would seem that, after deprotonation of coordinated aliphatic amino groups, the formation of the double bond between the α-carbon and the aliphatic amino nitrogens, the transfer of a proton from the α-carbon to coordinated dioxygen, the homolytic cleavage of the O–O bond, and the electron transfer from the ligand through the metal ion to the coordinated oxygen are concerted, as indicated by **8**. The transfer of a proton from

(26) Glasstone, S.; Laidler, L. J.; Eyring, H. *The Theory of Rate Processes*; McGraw-Hill: New York, 1941.
(27) Ealing Precision Molecular Models, CPK Space Filling Model; The Ealing Corp., South Natick, MA 01760.

Scheme I. Proposed Mechanism for the Oxidative Dehydrogenation of 1,6-Bis(2-pyridyl)2,5-diazahexane (PYEN) through Dioxygen Complex Formation

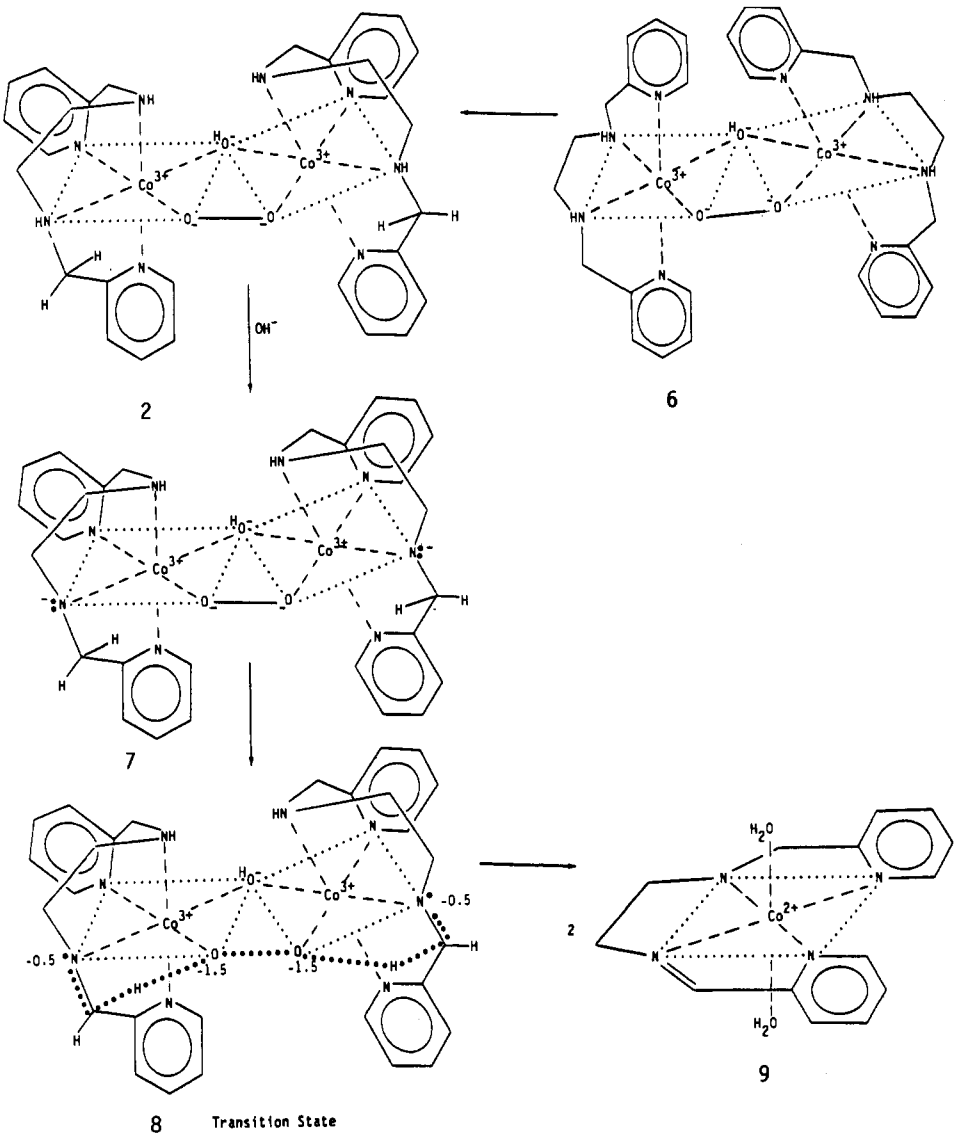

the α-carbon atom of the aminomethylene moiety of the ligand to the peroxo group indicated in the transition-state complex would seem to require a large deuterium isotope effect.

The suggested reaction mechanism illustrated in Scheme I, **2** → **7** → **8** → **9**, for the oxidative dehydrogenation of the coordinated PYEN applies to the oxidative dehydrogenation of **2**, the conformation that has been assigned the highest reactivity. Unreactive species such as **6** would presumably have to be converted to the more reactive species **2** or **3** before the reaction could proceed, in accordance with the reasoning presented above concerning the relative reactivities of the species in solution. A scheme for the direct conversion of **3** to the reaction products is not presented at this time because of the uncertainties about the conformation of the less reactive species in solution and the number of such species that may be present. The rates of degradation of the μ-peroxo-μ-hydroxo complex formed by 1,1,6,6-tetradeuteriated PYEN at three p[H] values gave ratios of $k_1^f(H)/k_1^f(D) = 8.2$ and $k_1^s(H)/k_1^s(D) = 7.4$. These large kinetic deuterium isotope effects seem to parallel the large isotope effects recently reported for oxidative dehydrogenation reactions of analogous dioxygen complexes[14] and primary hydrogen isotope effects of C–H bond breaking.[28,29]

The large primary kinetic isotope effect suggests that the transition state is probably of the type suggested by Eigen[30] in a "one encounter" or "intimate" mechanism in which both proton transfers (one from each α-carbon atom) take place in a single step. This suggests that in the transition state the proton being transferred is bound to the α-carbon of the ligand as well as to one oxygen atom of the peroxo bridge, thereby reducing the ground-state stretching frequencies of both C–H and O–H bonds.

The questions raised by the results of this and previous investigations of oxidative dehydrogenation of coordinated ligands by coordinated dioxygen are being investigated further in this laboratory by kinetic studies of this type of reaction in dioxygen complexes having ligands with a variety of geometrical conformations.

Acknowledgment is made to the donors of the Petroleum Research Fund, administered by the American Chemical Society, for support of this research. We express our thanks for helpful suggestions from David Stanbury, Auburn University, and Alan Sargeson, ANU, Canberra, Australia.

Registry No. $[Co_2(PYEN)_2O_2(OH)]^+$, 39019-67-5; PYEN, 4608-34-8; D_2, 7782-39-0.

(28) Kresge, A. J. *Isotope Effects in Enzyme Catalyzed Reactions*; Cleland, W. E., O'Leary, M. H., Northrop, D. B., Eds.; University Park Press: Baltimore, MD, 1977; p 37.

(29) Melander, L.; Saunders, W. H., Jr. *Reaction Rates of Isotopic Molecules*; Wiley: New York, 1980.

(30) Eigen, M. *Discuss. Faraday Soc.* **1965**, *39*, 7.